Investigating Diffusion Coefficient Using Dynamic Light Scattering Technique

Yong Sun*

February 2, 2008

Abstract

In this work, the Z-average, effective, apparent diffusion coefficients and their poly-dispersity indexes were investigated for dilute poly-disperse homogeneous spherical particles in dispersion where the Rayleigh-Gans-Debye approximation is valid. The results reveal that the values of the apparent and effective diffusion coefficients at a scattering angle investigated are consistent and the difference between the effective and Z-average diffusion coefficients is a function of the mean particle size, size distribution and scattering angle. For the small particles with narrow size distributions, the Z-average diffusion coefficient can be got directly at any scattering angle. For the small particles with wide size distributions, the Z-average diffusion coefficient should be measured at a small scattering angle. For large particles, in order to obtain a good approximate value of Z-average diffusion coefficient, the wider the particle size distribution, the smaller the scattering angle that the DLS data are measured. The poly-dispersity index of the effective diffusion coefficient at a scattering angle investigated is consistent with that of the Z-average diffusion coefficient and without considering the influences of noises, the difference between the poly-dispersity indexes of the Z-average and apparent diffusion coefficients is determined by the mean particle size, size distribution and scattering angle together.

1 INTRODUCTION

For colloidal dispersion systems, light scattering is a widely used technique to measure the characteristics of particles. One of the main applications of the dynamic light scattering (DLS) technique is to obtain the Z-average diffusion coefficient and its poly-dispersity index for particles in liquid suspension. The DLS technique is to measure the particle properties from the normalized time auto-correlation function of the scattered light $g^{(2)}(\tau)$, here τ is the correlation delay time. The moments (or Cumulants) method [1–4] has been used as a standard method to measure the Z-average diffusion coefficient and its poly-dispersity index from the DLS data. In general, when the DLS data are analyzed, the mean diffusion coefficient and its poly-dispersity index obtained

*Email: ysun2002h@yahoo.com.cn

using the moments method are the apparent diffusion coefficient and its poly-dispersity index.

About the relationship between the Z-average and apparent diffusion coefficients has been investigated by a few authors [3]. Under appropriate conditions, they measured the Z-average diffusion coefficient by fitting $ln\left(C^{1/2}\left|g^{(1)}(\tau)\right|\right)$ to linear, quadratic and cubic function of τ. The effective values of $\langle\Gamma\rangle$ and μ_2 obtained from the fits are plotted against $\langle\Gamma\rangle\tau_{max}$ and thus are obtained by extrapolating $\langle\Gamma\rangle\tau_{max}$ to 0, where $\langle\Gamma\rangle$ is the mean decay rate. Combining in the Svedberg equation with the weight-average sedimentation coefficient, the weight-average molar mass can be yielded. For large particles, the authors suggest the Z-average diffusion coefficient should be measured at a small enough scattering angle. In order to obtain the accurate value of the weight-average molar mass, it is important to measure the value of Z-average diffusion coefficient accurately.

In this work, the Z-average, effective, apparent diffusion coefficients and their poly-dispersity indexes were investigated for dilute poly-disperse homogeneous spherical particles in dispersion where the Rayleigh-Gans-Debye (RGD) approximation is valid. The results reveal that the values of the apparent and effective diffusion coefficients at a scattering angle investigated are consistent and the difference between the effective and Z-average diffusion coefficients is a function of the mean particle size, size distribution and scattering angle. For the small particles with narrow size distributions, the Z-average diffusion coefficient can be got directly at any scattering angle. For the small particles with wide size distributions, the Z-average diffusion coefficient should be measured at a small scattering angle. For large particles, in order to obtain a good approximate value of Z-average diffusion coefficient, the wider the particle size distribution, the smaller the scattering angle that the DLS data are measured. The poly-dispersity index of the effective diffusion coefficient at a scattering angle investigated is consistent with that of the Z-average diffusion coefficient and without considering the influences of noises, the difference between the poly-dispersity indexes of the Z-average and apparent diffusion coefficients is determined by the mean particle size, size distribution and scattering angle together. For narrow particle size distributions, they are consistent. For wide particle size distributions, the poly-dispersity index of apparent diffusion coefficient should be measured at a τ range where τ_{max} changes to a small value in order to obtain a good approximate result of the poly-dispersity index of Z-average diffusion coefficient.

2 THEORY

For dilute poly-disperse homogeneous spherical particles in dispersion where the RGD approximation is valid, the effective diffusion coefficient D_{eff} and its poly-dispersity index $\left(\frac{\sqrt{\mu_2}}{\langle\Gamma\rangle}\right)_{eff}$ obtained using the moments method at a given scattering vector as $\tau \to 0$ are given by

$$D_{eff} = \frac{\int_0^\infty R_s^6 P(qR_s) DG(R_s) dR_s}{\int_0^\infty R_s^6 P(qR_s) G(R_s) dR_s} \tag{1}$$

and

$$\left(\frac{\sqrt{\mu_2}}{\langle\Gamma\rangle}\right)_{eff} = \left(\frac{\int_0^\infty R_s^6 P\left(qR_s\right) D^2 G\left(R_s\right) dR_s \int_0^\infty R_s^6 P\left(qR_s\right) G\left(R_s\right) dR_s}{\left(\int_0^\infty R_s^6 P\left(qR_s\right) DG\left(R_s\right) dR_s\right)^2} - 1\right)^{1/2} \quad (2)$$

where R_s is the static radius, D is the diffusion coefficient, $q = \frac{4\pi}{\lambda} n_s \sin\frac{\theta}{2}$ is the scattering vector, λ is the wavelength of the incident light in vacuo, n_s is the solvent refractive index, θ is the scattering angle, μ_2 is the second moment, $G\left(R_s\right)$ is the number distribution of particles and the form factor $P\left(q, R_s\right)$ is

$$P\left(q, R_s\right) = \frac{9}{q^6 R_s^6} \left(\sin\left(qR_s\right) - qR_s \cos\left(qR_s\right)\right)^2. \quad (3)$$

If the scattering vector approximates 0, the Z-average diffusion coefficient D_z and its poly-dispersity index $\left(\frac{\sqrt{\mu_2}}{\langle\Gamma\rangle}\right)_z$ can be obtained

$$D_z = \frac{\int_0^\infty R_s^6 DG\left(R_s\right) dR_s}{\int_0^\infty R_s^6 G\left(R_s\right) dR_s} \quad (4)$$

and

$$\left(\frac{\sqrt{\mu_2}}{\langle\Gamma\rangle}\right)_z = \left(\frac{\int_0^\infty R_s^6 D^2 G\left(R_s\right) dR_s \int_0^\infty R_s^6 G\left(R_s\right) dR_s}{\left(\int_0^\infty R_s^6 DG\left(R_s\right) dR_s\right)^2} - 1\right)^{1/2}. \quad (5)$$

From the Einstein-Stokes relation, the diffusion coefficient D can be written as

$$D = \frac{k_B T}{6\pi\eta_0 R_h}, \quad (6)$$

where η_0, k_B, T and R_h are the viscosity of the solvent, Boltzmann's constant, absolute temperature and hydrodynamic radius, respectively.

In this work, the number distribution is chosen as a Gaussian distribution

$$G\left(R_s; \langle R_s\rangle, \sigma\right) = \frac{1}{\sigma\sqrt{2\pi}} \exp\left(-\frac{1}{2}\left(\frac{R_s - \langle R_s\rangle}{\sigma}\right)^2\right), \quad (7)$$

where $\langle R_s\rangle$ is the mean static radius and σ is the standard deviation related to the mean static radius.

3 RESULTS AND DISCUSSION

In the previous work [5, 6], it was shown that the expected values of the DLS data calculated based on the commercial and static particle size information are consistent with the experimental data. In order to investigate the quantities of D_z, D_{eff}, D_{app} and their ploy-dispersity indexes accurately, the values of $g^{(2)}\left(\tau\right)$ were produced as described in the previous work [5] and thus D_z, D_{eff} and their ploy-dispersity indexes are calculated using Eqs.1, 2, 4, 5 and D_{app} and its poly-dispersity index are obtained using the first two moments method, respectively.

The values of $g^{(2)}(\tau)$ were produced using the information: the temperature T, viscosity of the solvent η_0, wavelength of laser light λ, refractive index of the water n_s and constant R_h/R_s were set to 300.49K, 0.8479 mPa·S, 632.8 nm, 1.332 and 1.1 for $\langle R_s \rangle$ =50 nm, 1.2 for $\langle R_s \rangle$ =120 and 260 nm, scattering angle θ was chosen as 30° and 90° for $\langle R_s \rangle$ =50 and 120 nm and 30° for $\langle R_s \rangle$ =260 nm, and standard deviation σ was set to (3, 5, 10, 15, 20, 25)nm, (8, 12, 24, 36, 48, 60)nm and (16, 26, 52, 78, 104, 130)nm for $\langle R_s \rangle$ =50, 120 and 260 nm, respectively. When the data of $\left(g^{(2)}(\tau)-1\right)/\beta$ were obtained, the random errors were set 3%. In order to investigate the poly-dispersity indexes for narrow particle size distributions, the statistical noises were not added.

When the first two moments method were used to fit the simulated data, the values of Γ_{app} and μ_{2app} were chosen when they stabilize. The results for the simulated data produced based on the mean static radius 50 nm and standard deviations 5, 25 nm at scattering angles 30° and 90° were shown in Figs. 1 and 2, respectively. The results show that all the fit values obtained using the first two moments method are consistent with the simulated data very well, respectively.

The values of D_z and D_{eff} at scattering angles 30° and 90° for different standard deviations 3, 5, 10, 15, 20 and 25 nm were calculated using Eqs. 1 and 4 and the results of D_{app} are obtained using the first two moments method to fit the different simulated data, respectively. All results of D_z, D_{eff} and D_{app} for standard deviations 3, 15 and 25 nm are listed in Table 1.

$\sigma\,(nm)$	3		15		25	
$D_z\left(10^{-12}m^2/s\right)$	4.638		3.501		2.687	
θ	30°	90°	30°	90°	30°	90°
$D_{eff}\left(10^{-12}m^2/s\right)$	4.639	4.644	3.513	3.593	2.709	2.862
$D_{app}\left(10^{-12}m^2/s\right)$	4.634±0.002	4.646±0.008	3.507±0.002	3.592±0.007	2.703±0.001	2.861±0.006

Table 1: The values of D_z, D_{eff} and D_{app} for the simulated data produced based on the mean static radius 50 nm and standard deviations 3, 15 and 25 nm at scattering angles 30° and 90°, respectively.

Table 1 shows that the value of D_{eff} is consistent with that of D_{app} at any scattering angle investigated and the difference between the values of D_z and D_{eff} is influenced by the scattering angle and particle size distribution. For narrow particle size distributions, the value of D_z is consistent with that of D_{eff} obtained at any scattering angle investigated. For wide particle size distributions, the difference between them is a function of the scattering angle. At a small scattering angle, the result of D_{eff} is a good approximate value of D_z.

The values of $\left(\frac{\sqrt{\mu_2}}{\langle\Gamma\rangle}\right)_z$ and $\left(\frac{\sqrt{\mu_2}}{\langle\Gamma\rangle}\right)_{eff}$ at scattering angles 30° and 90° for different standard deviations 3, 5, 10, 15, 20 and 25 nm were calculated using Eqs. 2, 5 and the results of $\left(\frac{\sqrt{\mu_2}}{\langle\Gamma\rangle}\right)_{app}$ are obtained using the first two moments method to fit the different simulated data, respectively. All results of $\left(\frac{\sqrt{\mu_2}}{\langle\Gamma\rangle}\right)_z$, $\left(\frac{\sqrt{\mu_2}}{\langle\Gamma\rangle}\right)_{eff}$ and $\left(\frac{\sqrt{\mu_2}}{\langle\Gamma\rangle}\right)_{app}$

for standard deviations 3, 15 and 25 nm are listed in Table 2.

$\sigma\,(nm)$	3		15		25	
$\left(\sqrt{\mu_2}/\langle\Gamma\rangle\right)_z$	0.059		0.208		0.253	
θ	30^o	90^o	30^o	90^o	30^o	90^o
$\left(\sqrt{\mu_2}/\langle\Gamma\rangle\right)_{eff}$	0.059	0.059	0.208	0.209	0.253	0.255
$\left(\sqrt{\mu_2}/\langle\Gamma\rangle\right)_{app}$	0.058±0.006	0.059±0.009	0.198±0.003	0.200±0.008	0.236±0.002	0.238±0.006

Table 2: The values of $\left(\frac{\sqrt{\mu_2}}{\langle\Gamma\rangle}\right)_z$, $\left(\frac{\sqrt{\mu_2}}{\langle\Gamma\rangle}\right)_{eff}$ and $\left(\frac{\sqrt{\mu_2}}{\langle\Gamma\rangle}\right)_{app}$ for the simulated data produced based on the mean static radius 50 nm and standard deviations 3, 15 and 25 nm at scattering angles 30^o and 90^o, respectively.

Table 2 reveals that the value of $\left(\frac{\sqrt{\mu_2}}{\langle\Gamma\rangle}\right)_{eff}$ at any scattering angle investigated is consistent with that of $\left(\frac{\sqrt{\mu_2}}{\langle\Gamma\rangle}\right)_z$ and the difference between $\left(\frac{\sqrt{\mu_2}}{\langle\Gamma\rangle}\right)_{eff}$ and $\left(\frac{\sqrt{\mu_2}}{\langle\Gamma\rangle}\right)_{app}$ at a scattering angle investigated is affected by the particle size distribution. For narrow particle size distributions, they are consistent. For wide particle size distributions, the poly-dispersity index of apparent diffusion coefficient should be measured at a τ range where τ_{max} changes to a small value in order to obtain a good approximate result of the poly-dispersity index of Z-average diffusion coefficient.

Next, the simulated data produced based on the mean static radius 120 nm and standard deviations 8, 12, 24, 36, 48, 60 nm at scattering angles 30^o and 90^o were explored. The fit results for the simulated data produced based on the standard deviations 12 nm, 60 nm at scattering angles 30^o and 90^o are shown in Figs. 3 and 4, respectively. The figures show that all the fit values obtained using the first two moments method represent the simulated data very well, respectively.

In order to obtain the results of D_{eff} at scattering angles 30^o and 90^o, and D_z, the mean static radius 120 nm and standard deviations 8, 12, 24, 36, 48, 60 nm were input into Eqs. 1 and 4 to calculate and the results of D_{app} are measured using the first two moments method to fit the different simulated data, respectively. All results of D_z, D_{eff} and D_{app} for standard deviations 8, 36 and 60 nm are shown in Table 3.

$\sigma\,(nm)$	8		36		60	
$D_z\left(10^{-12}m^2/s\right)$	1.765		1.337		1.026	
θ	30^o	90^o	30^o	90^o	30^o	90^o
$D_{eff}\left(10^{-12}m^2/s\right)$	1.767	1.783	1.364	1.588	1.077	1.476
$D_{app}\left(10^{-12}m^2/s\right)$	1.765±0.001	1.784±0.002	1.362±0.001	1.587±0.002	1.075±0.001	1.476±0.002

Table 3: The values of D_z, D_{eff} and D_{app} for the simulated data produced based on the mean static radius 120 nm and standard deviations 8, 36 and 60 nm at scattering angles 30^o and 90^o, respectively.

Table 3 shows clearly the influences of particle size distribution on the results of D_{eff}

and D_{app}. For narrow particle size distributions, the values of D_{eff} and D_{app} obtained at any scattering angle investigated are consistent with that of D_z. For wide particle size distributions, the values of D_{app} and D_{eff} obtained at a scattering angle investigated still are consistent and the difference between D_z and D_{eff} depends on the scattering angle. In order to get the good approximate value of D_z, the fit results of D_{app} should be obtained at a small scattering angle.

The values of $\left(\frac{\sqrt{\mu_2}}{\langle\Gamma\rangle}\right)_z$ and $\left(\frac{\sqrt{\mu_2}}{\langle\Gamma\rangle}\right)_{eff}$ at scattering angles 30° and 90° for different standard deviations 8, 12, 24, 36, 48, 60 nm were calculated using Eqs. 2, 5 and the results of $\left(\frac{\sqrt{\mu_2}}{\langle\Gamma\rangle}\right)_{app}$ are obtained using the first two moments method to fit the different simulated data, respectively. All results listed in Table 4 show the value of $\left(\frac{\sqrt{\mu_2}}{\langle\Gamma\rangle}\right)_{eff}$ obtained at any scattering angle is consistent with that of $\left(\frac{\sqrt{\mu_2}}{\langle\Gamma\rangle}\right)_z$ and the difference between $\left(\frac{\sqrt{\mu_2}}{\langle\Gamma\rangle}\right)_{eff}$ and $\left(\frac{\sqrt{\mu_2}}{\langle\Gamma\rangle}\right)_{app}$ is affected by the particle size distribution. For narrow particle size distributions, they are consistent. For wide particle size distributions, the poly-dispersity index of apparent diffusion coefficient should be measured at a τ range where τ_{max} changes to a small value in order to obtain a good approximate result of the poly-dispersity index of Z-average diffusion coefficient.

$\sigma\,(nm)$	8		36		60	
$\left(\sqrt{\mu_2}/\langle\Gamma\rangle\right)_z$	0.065		0.208		0.253	
θ	30°	90°	30°	90°	30°	90°
$\left(\sqrt{\mu_2}/\langle\Gamma\rangle\right)_{eff}$	0.065	0.065	0.209	0.208	0.254	0.258
$\left(\sqrt{\mu_2}/\langle\Gamma\rangle\right)_{app}$	0.065±0.005	0.065±0.008	0.199±0.002	0.196±0.003	0.237±0.002	0.246±0.003

Table 4: The values of $\left(\frac{\sqrt{\mu_2}}{\langle\Gamma\rangle}\right)_z$, $\left(\frac{\sqrt{\mu_2}}{\langle\Gamma\rangle}\right)_{eff}$ and $\left(\frac{\sqrt{\mu_2}}{\langle\Gamma\rangle}\right)_{app}$ for the simulated data produced based on the mean static radius 120 nm and standard deviations 8, 36 and 60 nm at scattering angles 30° and 90°, respectively.

Finally, the situations for much larger particles were investigated. The simulated data produced based on the mean static radius 260 nm and standard deviations 16, 26, 52, 78, 104, 130 nm at a scattering angle of 30° were explored. The fit results for the simulated data produced based on the standard deviations 26 nm, 130 nm at scattering angles 30° were shown in Fig. 5a and 5b, respectively. Figure 5 shows that all the fit values obtained using the first two moments method are consistent with the simulated data very well, respectively.

As above, using Eqs. 1 and 4, the values of D_z and D_{eff} at a scattering angle of 30° for different standard deviations 16, 26, 52, 78, 104, 130 nm were obtained and using the first two moments method to fit the different simulated data, the results of D_{app} are got, respectively. All the results of D_z, D_{eff} and D_{app} for the standard deviations 16, 26, 78, 104 and 130 nm are listed in Table 5.

Table 5 reveals the same results as Tables 1 and 3. For narrow particle size distributions, the values of D_{eff} and D_{app} obtained at a scattering angle of 30° are consistent

$\sigma\,(nm)$	16	26	78	104	130
$D_z\,(10^{-13}m^2/s)$	8.170	7.940	6.173	5.383	4.742
$D_{eff}\,(10^{-13}m^2/s)$	8.212	8.047	6.835	6.366	6.039
$D_{app}\,(10^{-13}m^2/s)$	8.203±0.004	8.037±0.004	6.821±0.004	6.350±0.003	6.021±0.003

Table 5: The values of D_z, D_{eff} and D_{app} for the simulated data produced based on the mean static radius 260 nm and standard deviations 16, 26, 78, 104 and 130 nm at a scattering angle of 30°.

with that of D_z. For a wide particle size distribution, the results of D_{app} and D_{eff} still are consistent and the values of D_z and D_{eff} can have a large difference. In order to get the good approximate value of D_z, the DLS data for wide particle size distributions should be measured at a much smaller scattering angle.

Using Eqs. 2, 5, the values of $\left(\frac{\sqrt{\mu_2}}{\langle\Gamma\rangle}\right)_z$ and $\left(\frac{\sqrt{\mu_2}}{\langle\Gamma\rangle}\right)_{eff}$ at a scattering angle of 30° for different standard deviations 16, 26, 78, 104, 130 nm were calculated and using the first two moments method to fit the different simulated data, the results of $\left(\frac{\sqrt{\mu_2}}{\langle\Gamma\rangle}\right)_{app}$ are obtained, respectively. All results listed in Table 6 show the same results as Table 2 and 4. The value of $\left(\frac{\sqrt{\mu_2}}{\langle\Gamma\rangle}\right)_{eff}$ is consistent with that of $\left(\frac{\sqrt{\mu_2}}{\langle\Gamma\rangle}\right)_z$ and the difference between $\left(\frac{\sqrt{\mu_2}}{\langle\Gamma\rangle}\right)_{eff}$ and $\left(\frac{\sqrt{\mu_2}}{\langle\Gamma\rangle}\right)_{app}$ is affected by the particle size distribution. For narrow particle size distributions, they are consistent.

$\sigma\,(nm)$	16	26	78	104	130
$\left(\sqrt{\mu_2}/\Gamma\right)_z$	0.060	0.094	0.208	0.235	0.252
$\left(\sqrt{\mu_2}/\Gamma\right)_{eff}$	0.060	0.095	0.211	0.236	0.250
$\left(\sqrt{\mu_2}/\Gamma\right)_{app}$	0.060±0.005	0.094±0.004	0.200±0.002	0.221±0.002	0.231±0.002

Table 6: The values of $\left(\frac{\sqrt{\mu_2}}{\langle\Gamma\rangle}\right)_z$, $\left(\frac{\sqrt{\mu_2}}{\langle\Gamma\rangle}\right)_{eff}$ and $\left(\frac{\sqrt{\mu_2}}{\langle\Gamma\rangle}\right)_{app}$ for the simulated data produced based on the mean static radius 260 nm and standard deviations 16, 26, 78, 104 and 130 nm at a scattering angle of 30°.

In order to explore the influences of a wide particle size distribution on D_{eff} for small particles in details, the values of D_{eff} were calculated using Eq. 1 for $\langle R_s\rangle$ 30 nm and σ 15 nm at different scattering angles. All results are shown in Fig. 6. Figure 6 reveals clearly that the DLS data should be measured at a small scattering angle in order to obtain a good approximate value of D_z.

4 CONCLUSION

The values of the apparent and effective diffusion coefficients at a scattering angle investigated are consistent and the difference between the effective and Z-average diffusion coefficients is a function of the mean particle size, size distribution and scattering angle.

For the small particles with narrow size distributions, the Z-average diffusion coefficient can be got directly at any scattering angle. For the small particles with wide size distributions, the Z-average diffusion coefficient should be measured at a small scattering angle. For large particles, in order to obtain a good approximate value of Z-average diffusion coefficient, the wider the particle size distribution, the smaller the scattering angle that the DLS data are measured. The poly-dispersity index of the effective diffusion coefficient at a scattering angle investigated is consistent with that of the Z-average diffusion coefficient and without considering the influences of noises, the difference between the poly-dispersity indexes of the Z-average and apparent diffusion coefficients is determined by the mean particle size, size distribution and scattering angle together. For narrow particle size distributions, they are consistent. For wide particle size distributions, the poly-dispersity index of apparent diffusion coefficient should be measured at a τ range where τ_{max} changes to a small value in order to obtain a good approximate result of the poly-dispersity index of Z-average diffusion coefficient.

Fig. 1 The fit results of $g^{(2)}(\tau)$ for the simulated data produced based on the mean static radius 50 nm and standard deviation 5 nm. The circles show the simulated data and the line represents the fit results obtained using the first two moments method. The results for scattering angles 30^o and 90^o are shown in a and b, respectively.

Fig. 2 The fit results of $g^{(2)}(\tau)$ for the simulated data produced based on the mean static radius 50 nm and standard deviation 25 nm. The circles show the simulated data and the line represents the fit results obtained using the first two moments method. The results for scattering angles 30^o and 90^o are shown in a and b, respectively.

Fig. 3 The fit results of $g^{(2)}(\tau)$ for the simulated data produced based on the mean static radius 120 nm and standard deviation 12 nm. The circles show the simulated data and the line represents the fit results obtained using the first two moments method. The results for scattering angles 30^o and 90^o are shown in a and b, respectively.

Fig. 4 The fit results of $g^{(2)}(\tau)$ for the simulated data produced based on the mean static radius 120 nm and standard deviation 60 nm. The circles show the simulated data and the line represents the fit results obtained using the first two moments method. The results for scattering angles 30^o and 90^o are shown in a and b, respectively.

Fig. 5 The fit results of $g^{(2)}(\tau)$ for the simulated data produced based on the mean static radius 260 nm and standard deviations 26 and 130 nm. The circles show the simulated data and the line represents the fit results obtained using the first two moments method. The results for standard deviations 26 and 130 nm are shown in a and b, respectively.

Fig. 6 The values of D_{eff} for the simulated data produced based on the mean static radius 30 nm and standard deviation 15 nm at different scattering angles.

References

[1] D. E. Koppel, J. Chem. Phys. **57**, 4814(1972).

[2] C. B. Bargeron, J. Chem. Phys. **61**, 2134(1974).

[3] J. C. Brown, P. N. Pusey and R. Dietz, J. Chem. Phys. **62**, 1136(1975).

[4] B. J. Berne and R. Pecora, *Dynamic Light Scattering* (Robert E. Krieger Publishing Company, Malabar, Florida, 1990).

[5] Y. Sun arxiv.org/abs/physics/0511159.

[6] Y. Sun arxiv.org/abs/physics/0511160.

a).

Fig. 3

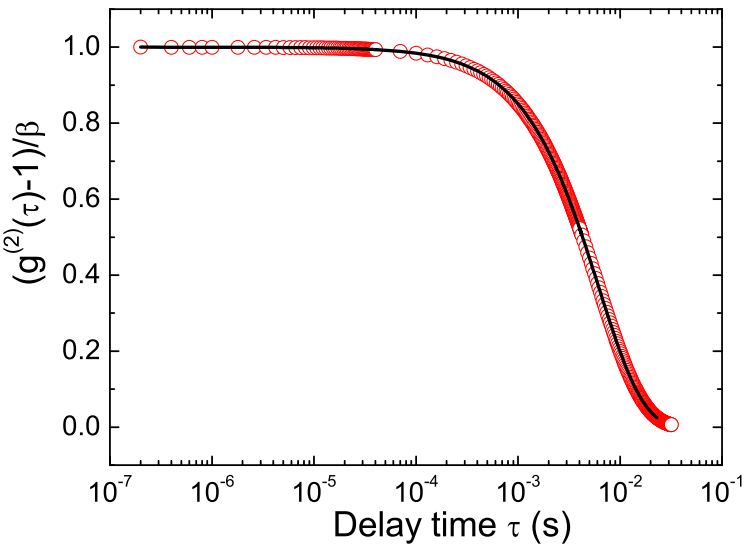

Fig. 4

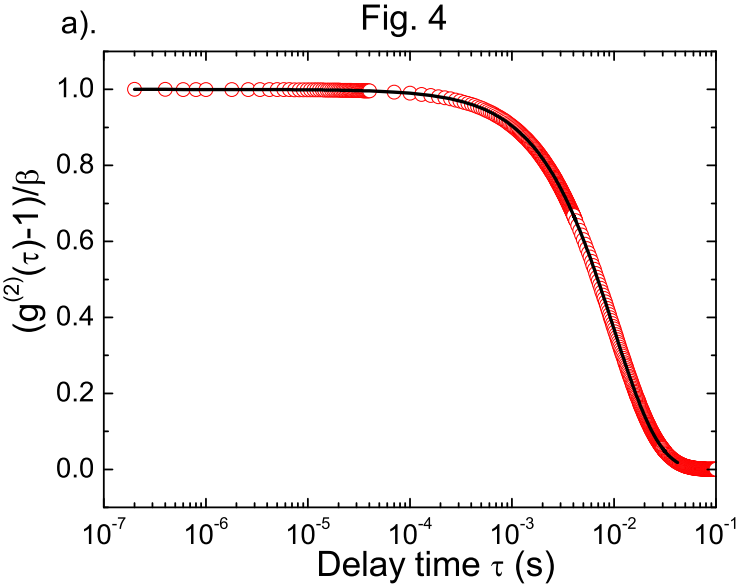
a).
1.0
0.8
0.6
0.4
0.2
0.0
$(g^{(2)}(\tau)-1)/\beta$
10^{-7}
10^{-6}
10^{-5}
10^{-4}
10^{-3}
10^{-2}
10^{-1}
Delay time τ (s)

b).

Fig. 3

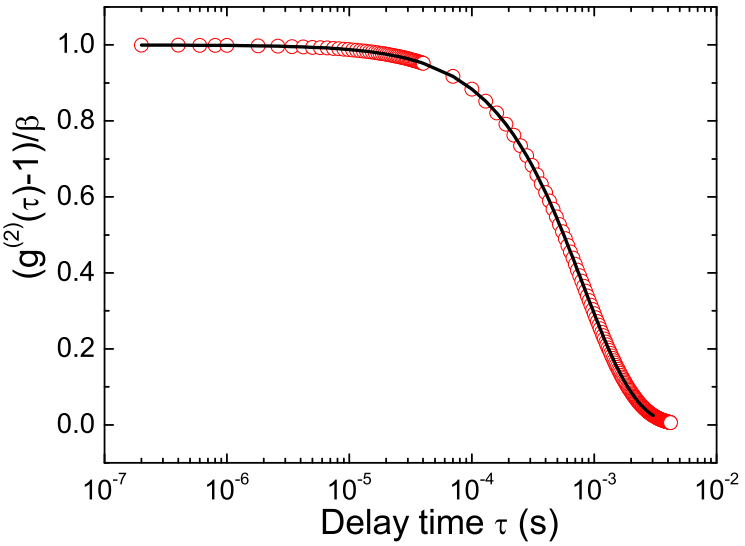
1.0
0.8
0.6
0.4
0.2
0.0
$(g^{(2)}(\tau)-1)/\beta$
10^{-7}
10^{-6}
10^{-5}
10^{-4}
10^{-3}
10^{-2}
Delay time τ (s)

Fig. 4

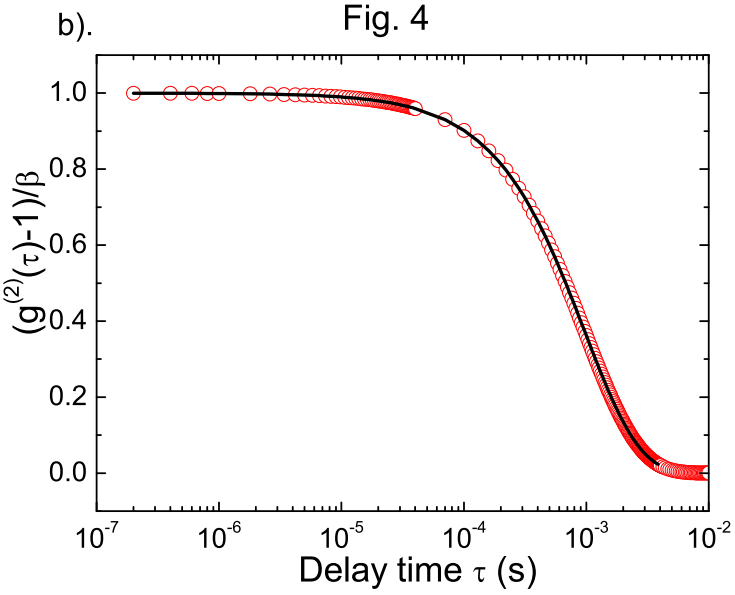
b).
1.0
0.8
0.6
0.4
0.2
0.0
$(g^{(2)}(\tau)-1)/\beta$
10^{-7}
10^{-6}
10^{-5}
10^{-4}
10^{-3}
10^{-2}
Delay time τ (s)

b).

Fig. 5

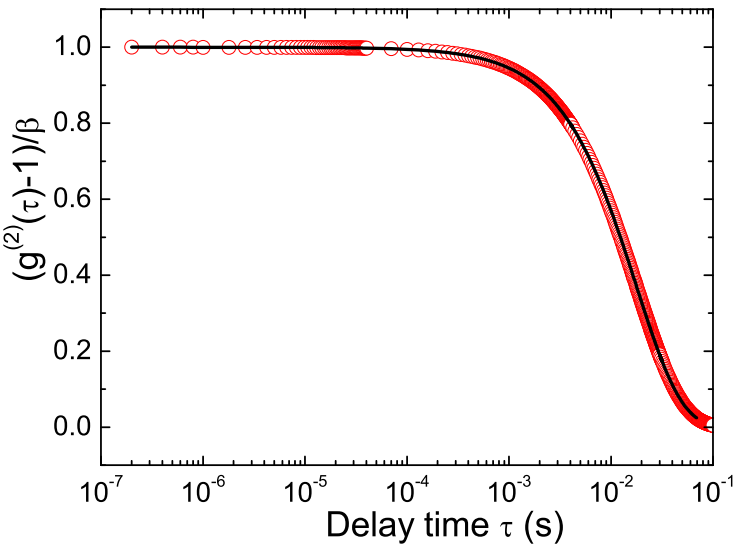
1.0
0.8
0.6
0.4
0.2
0.0
$(g^{(2)}(\tau)-1)/\beta$
10^{-7}
10^{-6}
10^{-5}
10^{-4}
10^{-3}
10^{-2}
10^{-1}
Delay time τ (s)

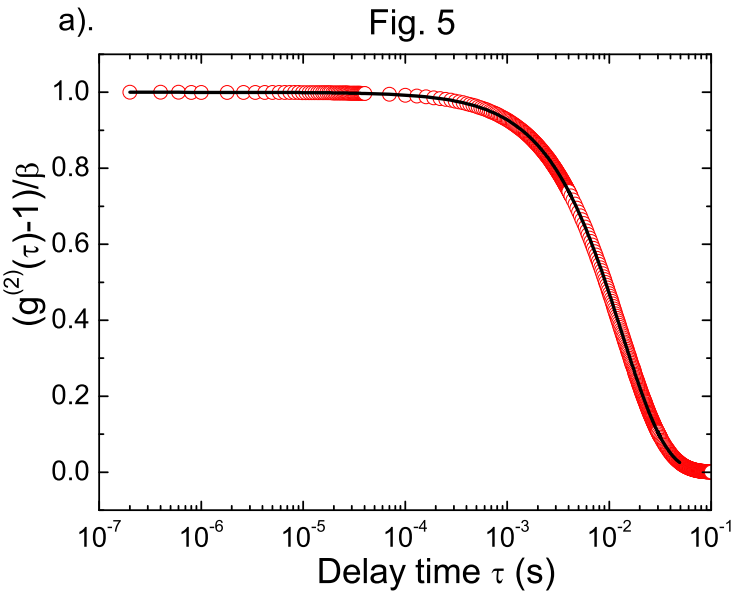
a).
Fig. 5
1.0
0.8
0.6
0.4
0.2
0.0
(g(2)(τ)-1)/β
10-7
10-6
10-5
10-4
10-3
10-2
10-1
Delay time τ (s)

a).

Fig. 2

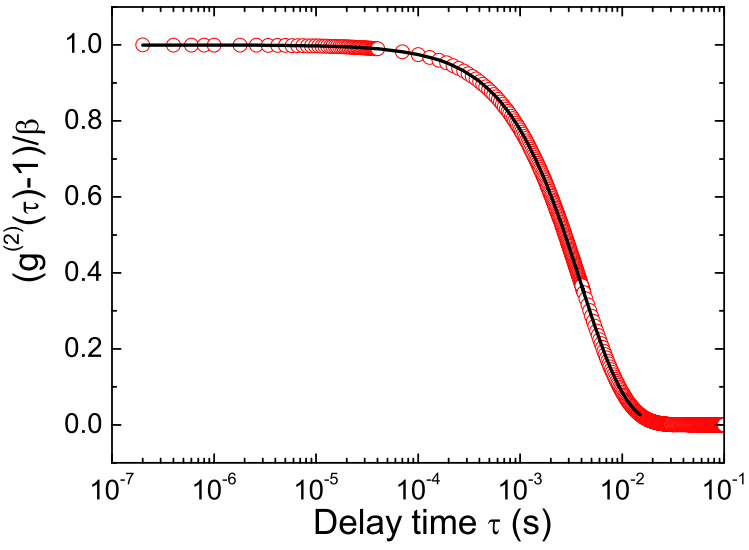
1.0
0.8
0.6
0.4
0.2
0.0
$(g^{(2)}(\tau)-1)/\beta$
10^{-7}
10^{-6}
10^{-5}
10^{-4}
10^{-3}
10^{-2}
10^{-1}
Delay time τ (s)

a).

Fig. 1

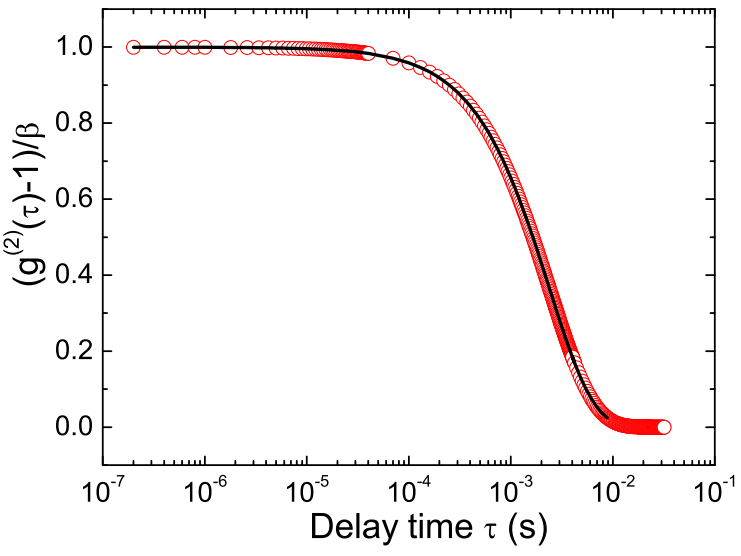
1.0
0.8
0.6
0.4
0.2
0.0
$(g^{(2)}(\tau)-1)/\beta$
10^{-7}
10^{-6}
10^{-5}
10^{-4}
10^{-3}
10^{-2}
10^{-1}
Delay time τ (s)

b).

Fig. 2

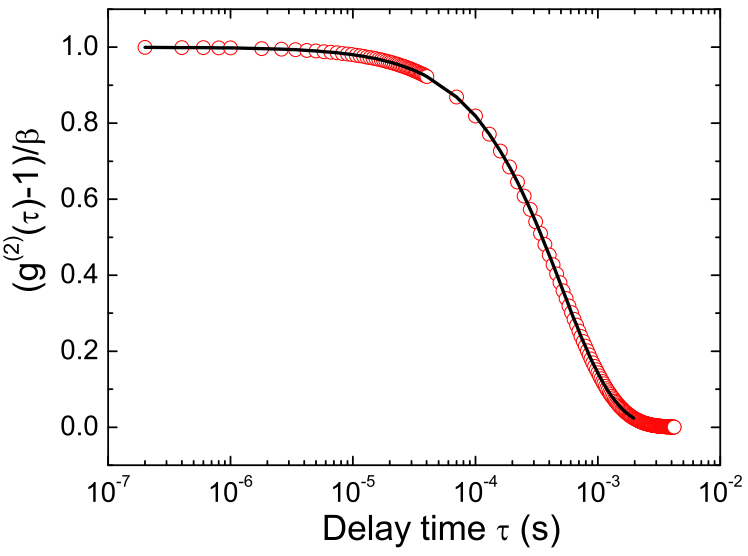
1.0
0.8
0.6
0.4
0.2
0.0
$(g^{(2)}(\tau)-1)/\beta$
10^{-7}
10^{-6}
10^{-5}
10^{-4}
10^{-3}
10^{-2}
Delay time τ (s)

b).

Fig. 1

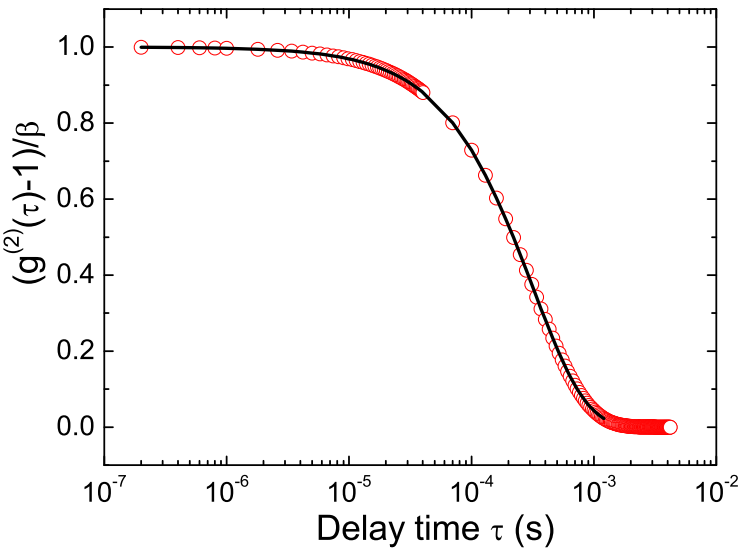
1.0
0.8
0.6
0.4
0.2
0.0
$(g^{(2)}(\tau)-1)/\beta$
10^{-7}
10^{-6}
10^{-5}
10^{-4}
10^{-3}
10^{-2}
Delay time τ (s)

Fig. 6

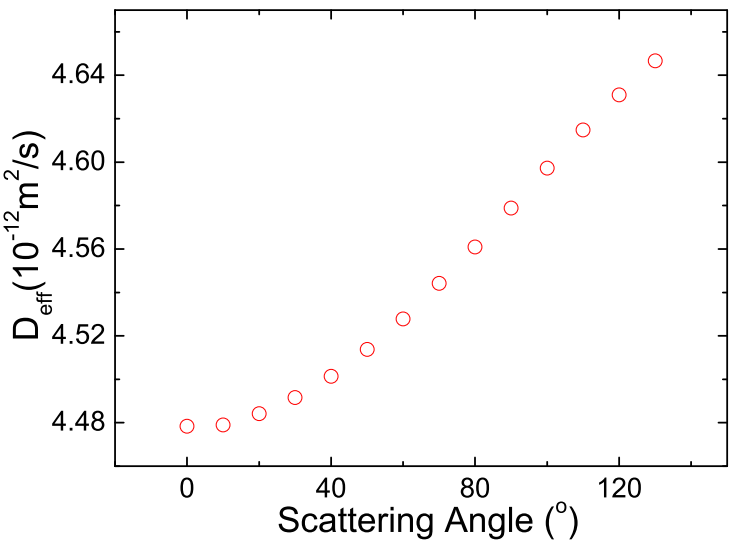
4.64
4.60
4.56
4.52
4.48
$D_{eff}(10^{-12}m^2/s)$
0
40
80
120
Scattering Angle (^{o})